# Automatic level set based cerebral vessel segmentation and bone removal in CT angiography data sets

Stephanie Behrens

Department of Simulation and Graphics, University of Magdeburg, Germany

**Abstract.** Computed tomography angiography (CTA) data sets without hardware based bone subtraction have the disadvantage of containing the bone structures which particularly overlap with vessel intensities; therefore vessel segmentation is hampered. Segmentation methods developed for CTA without bones can not handle these data sets and manual cerebral vessel segmentation is not realizable in clinical routines. Therefore, an automatic intensity based cerebral bone removal with subsequent edge based level set vessel segmentation method is presented in this work. [1]

## 1 Introduction

A continuously increasing incidence of vascular diseases implies a rising quantity of angiographic data sets (MRA - magnetic resonance angiography, CTA) and therewith a time consuming evaluation for radiologists and medical scientists. Manual extraction of vessels in a 3d data set is an arduous and imprecise process. Therefore, an accurate and automated vessel segmentation method would be a considerable assistance for clinical diagnosis, quantitative analysis of vascular diseases and computer-assisted detection (CAD), but designing an automatic segmentation method for CTA data sets is still a challenging problem due to the complex structure of the vascular system, noise, gaps in object boundaries and an overlapping intensity distribution of vessels to other structures.

Using a simple threshold or region growing based technique results in good vessel segmentations in MRA data sets, though due to by contrast agent enhanced vessels an intensity overlap between small bones, cartilage and vessels occurs, whereby these techniques are inapplicable for CTA data sets. Therefore bone removal as preprocessing step is indispensable for an explicit background suppression.

Hardware based methods for bone removal like presented in [7] and their disadvantages are widely discussed in literature, though only a few approaches for software based bone masking were introduced [5],[6]. Kanitsar et al.[5] present a system for peripheral bone removal by dividing the data sets into "slabs" and filter them with three thresholds subsequent by a connectivity-analysis. In

[1] recommended for submission to YRF2012 by Klaus D. Tönnies

normal cases there are no intensities overlaps due to the bone thickness and they vary only marginal in size, shape and thickness. Therefore, peripheral bone removal is simplified compared to intra cranial bone segmentation.

Another approach was presented by Kostopoulos et al. [6]. A two level decision tree was designed: first bones were distinguished from “vessel & parenchyma” followed by a differentiation between vasculature and parenchyma. The classification is based on a manually trained pixel-based classification algorithm. Training of a classifier algorithm is a tedious and protracted work and an adequate amount of samples is indispensable. Questionable is a successful training and classification for slices containing parts of the skull base, since the paper presents only a result for slices above the skull base.

Simple methods like thresholds, region growing or edge detection require homogeneous objects and closed object boundaries what is not given in CTA data sets. In contrast more complex methods like e.g. statistical models necessitate extensive apriori knowledge and user interaction. The software based approach presented in this paper will give reliable results for automatic bone removal in CTA data sets even in areas around the skull base. Due to the aforementioned properties of vasculature deformable models are the best choice for the use in vessel segmentation. Many approaches therefore can be found in literature like in [1]; [3], but level set based techniques ([8]) offer a multiplicity of advantages, the most important one being a topology-free representation. In Manniesing et al. [7] a level set algorithm is used for vessel segmentation with prior hardware based bone masking. Two intensity based speed functions were constructed for classifying edges to detect vessels. Using data sets with subtracted bones and by user placed seed points reduces the complexity for a vessel segmentation algorithm, in contrast in this work a solution for automatic software based bone removal subsequent by vessel segmentation is presented.

## 2 Method

The vessel segmentation method is divided into three steps: 1. bone removal, 2. initial model construction, 3. speed function calculation and level set vessel segmentation.

### 2.1 Bone removal

The challenge in CTA bone removal is the intensity overlap of around 200 HU values of bony structures (200HU up to 4000HU) and contrast enhanced blood vessels (100-400HU). Especially the area around the skull base contains a multiplicity of small bones and cartilage where the intensity overlap reaches its maximum. Furthermore, vasculature can be located close to bones and be completely enclosed by them so that their rim potentially disappears. Reducing this behaviour is desirable and a requirement for the level set method. The preprocessing is organised in three sub steps: 1. edge enhancement, 2. bone segmentation and 3. bone masking.

In the first step we aim to enhance light edges for a simplification of the distinction between small bones and blood vessels. The edges are enhanced by morphological gradients which can be manipulated by a structural element (SE) [9]:

$$p_{n_{SE}}B = \delta_{n_{SE}}B - \omega_{n_{SE}}B \tag{1}$$

the $\delta_{n_{SE}}B$ describing the dilation with a SE of size $n$ and $\omega_{n_{SE}}B$ defines the erosion of size $n$. Afterwards, an area closing filter is applied to fill the areas inside the bones or vessels.

In the second step the bones are segmented on $p_{n_{SE}}B$. For bone segmentation a classification of three different intensity overlapping types of tissues is required: vessels, bones or cartilage and background. Using a simple threshold method results in under-/ or over segmentation due to the intensity overlap. This problem can be solved by the double threshold technique DBLT [9]. Four threshold values in two ranges are set: $t_1$ and $t_4$ as the wide range containing all intensities of the desired object and $t_2$ and $t_3$ forming the narrow range with the overlapping intensities:

$$DBLT_{[t_1 \leq t_2 \leq t_3 \leq t_4]}(f) = R^{\delta}_{T_{[t_1,t_4](f)}}[T_{[t_2,t_3]}(f)], \tag{2}$$

with $f$ as input and $R^{\delta}_{T}(f)$ as morphological reconstruction. Bone and rim of bone voxels can be thereby segmented without affecting the blood vessel voxels. In the last step, the input is masked with the segmented bones, so that vessels and background remains.

### 2.2 Vessel segmentation

The initial model contains blood vessels and small parts of bony structures. Since no additionally manual placed seed points are used, it is important that the initial level set contains a rough segmentation of the cerebral vasculature to guarantee that the level set converges to a accurate solution.

The remaining non-vessel tissue features similar intensity values like the vessel voxels whereby an intensity based level set method is inapplicable and due to the created explicit object/background classification, an edge based level set approach was chosen. The level set vessel segmentation is divided in two steps: 1. edge preserving diffusion filtering for noise reduction; 2. Speed function construction and level set calculation.

The canny edge operator has been proven usefully to detect image edges, even light ones, independent from orientation or thickness. Small vessels and their rims can be therefore detected, whereby the canny filter the is best choice for this application and is applied to the diffusion filtered data set for speed function calculation. Speed functions are commonly build of three terms: the advection term to regulate the expansion in direction of extracted image features; the propagation term to control the expansion speed and the curvature term for a smooth solution. The used speed function was chosen in the following form:

$$I_{Canny(t)} = -\alpha(DT\nabla DT)\nabla I_{Canny} - \beta DT\,|\nabla I_{Canny}| + \epsilon\kappa_M\,|\nabla I_{Canny}|\,, \tag{3}$$

whereby $I_{Canny}$ represents the canny edge volume, $t$ the time step, $DT$ a distance transformation, $\kappa_M$ a mean curvature and $\alpha, \beta, \epsilon$ are weighting constants.

The DT inside the advection term regulates the distance between the actual level set and detected canny edges and represents a stopping criterion. For bridging gaps the DT is included into the propagation term as well. Starting from the initial level set the surface expands in the direction of the detected canny edges, whereupon the speed will be highly reduced at the edges. The propagation term prevents a leakage of the surface where no edges have been detected and is therefore, able to link associated vessels. Thus, the rough vessel segmentation can be optimised.

## 3 Parametrisation and evaluation

The presented method was evaluated on 6 clinical CTA data sets. Comparison was restricted to the relevant parts and done on 20-40 slices containing parts of the jawbones and skull base ($jb$) and parts of the Circle of Willis ($CoW$). For evaluation 3 CTA sets were manually segmented by an experienced user and 3 data sets were registered to an MRA data set, that was manually segmented by thresholding. Ground truth is not available for clinical data, therefore manual segmentation was chosen, though the accuracy is strongly dependent on the user. In many cases the user segments over the viewable rim of vessels.

The method was implemented with ITK [4] functions and all data sets were tested with a set of default and optimised parameter values (for parameter details, see section 2). The optimised values were found within experimental tests. For preprocessing the size of the structural element ($n_{SE}$) and the size for the area closing filter $\lambda$ have to be set. By default $t_1, t_2, t_3$ and $t_4$ were set to the average minimal values for bones ($t_1 = 250$), the average minimal values for bone boundaries ($t_2 = 350$), the average maximum bone boundary values ($t_3 = 800$) and the maximum intensity value of each data set ($t_4 = max(I)$). The speed

| Modality | Preprocessing | | | | | Canny detection | | Level set function | | |
|---|---|---|---|---|---|---|---|---|---|---|
| | $n_{SE}$ | $\lambda$ | $t_1$ | $t_2$ | $t_3$ | $\sigma^2$ | $thr_c$ | $\alpha$ | $\beta$ | Iso |
| CTA 1 (jb) | 2 | 150-360 | 230-390 | 290-450 | 600-800 | 0.05-0.1 | 5-50 | -3-(-8) | -7-(-15) | 110-250 |
| CTA 1 (CoW) | 3 | 300-750 | 250-380 | 350-550 | 800-120 | 0.05-0.08 | 5-45 | -4-(-8) | -8-(-15) | 127-220 |

**Table 1.** Parameter range for preprocessing and level set segmentation on CTA data sets.

function calculation of the level set segmentation is based on the canny threshold value $thr_c$ [2](controlling the length of the detected edges) and the variance $\sigma^2$ (size of smoothing filter). The values for $\sigma^2 = 0.05$ and $thr_c = 20$ were chosen

[2] Only the upper threshold has to be set, the lower threshold is automatically set $thr_L = thr_U/2$

to detect smaller vessels as well. According to a good initial model and a sensitive canny filter the constants $\alpha$ and $\beta$ were set to -8 and -10. The level set segmentation is controlled by the number of iterations $\#It = 100$ and in ITK an iso-surface $Iso$ value has to be set which defines the relevant intensities. With a default value of 137 even small vessels will be considered. All parameter values are summarized in table 1.

The dice coefficient and the conformity score [2] were used as evaluation measures, whereby the conformity score measures the quantity of false segmented voxels at a fraction of correct segmented voxels. The results are given in table 2. Visual inspection showed that the majority of vessels were segmented correctly and only a small amount of bony structures were left (see 1(a) and 1(b)). The double threshold method worked well for data sets with vessel HU between 200 and 400, finding the suitable threshold values for higher intensities is challenging. Bones enclosing vessels can be segmented, if vessel and surrounding bone intensities differ less than 50 HU, vessels were segmented as well. Optimised parameter values gave in all cases better results due to a higher amount of segmented jawbones and remained vessels.

The arduousness of manual segmentation reduced the evaluation results (see figure 1(c)). Some segmentation errors were induced by isolated thin bony structures, due to a high intensity overlap with vessel voxels and a missing connection to bones. Additionally, diffuse edges occurred in the registered data sets hampers the canny edge detection and the level set expansion. High vessel HU values caused by stenosis or stents increases the intensity overlap and complicates the initial model construction (like in CTA 6). The low concordance of CTA 5 is based on unusual low HU vessel values whereby the reference contains only an aneurysma.

## 4 Conclusion

The focus of this work was the development of a reliable bone removal technique for CTA data sets and a vessel segmentation. This was done by an intensity based preprocessing using the double threshold operator. The vessel segmentation is thereby simplified and an edge based level set vessel segmentation is used which produces good results. The presented method works automatically and by using the default parameter no user interaction is needed and parameter optimisation leads to slightly better results. The method can be used for MRA vessel segmentation as well. Automated parameter estimation would be desirable for the

| | CTA 1 | | CTA 2 | | CTA 3 | | CTA 4 | | CTA 5 | | CTA 6 | | MRA 1 | |
|---|---|---|---|---|---|---|---|---|---|---|---|---|---|---|
| | $Jb$ | $CoW$ | $Jb$ | $CoW$ | $Jb$ | $CoW$ | $Jb$ | $CoW$ | $Jb$ | $CoW$ | $Jb$ | $CoW$ | $Jb$ | $CoW$ |
| Dice | 50 | 61 | 53 | 70 | 61 | 70 | 46 | 2,8 | 12 | 53 | 24 | 42 | 73 | 42 |
| Conformity | -200 | -123 | -176 | -84 | -126 | -83 | -231 | -6800 | -1300 | -171 | -609 | -270 | -70 | -179 |

**Table 2.** Evaluation results for optimal parameter in %.

future. For the removal of isolated small-sized bony structures and the detection of pathological vessels apriori knowledge or user interaction would be a suitable method.

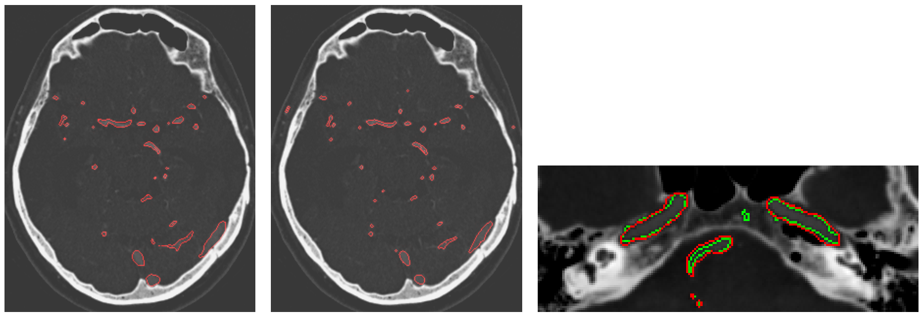

(a) Manual segmentation. (b) Level set segmentation. (c) Comparison of manual and level set segmentation.

**Fig. 1.** Comparison of level set and manual segmentation on CTA slices.

## References


1. van Bemmel, C., Spreeuwers, L., Viergever, M., Niessen, W.: Level-set-based artery-vein separation in blood pool agent CE-MR angiograms. Medical Imaging, IEEE Transactions on 22(10), 1224–1234 (2003)
2. Bogunovic, H., Pozo, J., Villa-Uriol, M.e.a.: Automated segmentation of cerebral vasculature with aneurysms in 3dra and tof-mra using geodesic active regions: an evaluation study. Medical Physics-New York-Institute of Physics 38(1) (2011)
3. Deschamps, T., Schwartz, P., Trebotich, D., Colella, P., Saloner, D., Malladi, R.: Vessel segmentation and blood flow simulation using level-sets and embedded boundary methods. In: International Congress Series. vol. 1268, pp. 75–80. Elsevier (2004)
4. Ibanez, L., Schroeder, W., Ng, L., Cates, J., et al.: The itk software guide. Kitware Inc (2005)
5. Kanitsar, A., Fleischmann, D., Wegenkittl, R.e.a.: Computed tomography angiography: a case study of peripheral vessel investigation. In: Proceedings of the conference on Visualization'01. pp. 477–480. IEEE Computer Society (2001)
6. Kostopoulos, S., Glotsos, D., Kagadis, G.e.a.: Development of a brain blood vessel segmentation method in ct-angiography (2005)
7. Manniesing, R., Velthuis, B., van Leeuwen et al., M.: Level set based cerebral vasculature segmentation and diameter quantification in ct angiography. Medical Image Analysis 10(2), 200–214 (2006)
8. Osher, S., Sethian, J.: Fronts propagating with curvature-dependent speed: algorithms based on Hamilton-Jacobi formulations. Journal of computational physics 79(1), 12–49 (1988)
9. Soille, P.: Morphological image analysis: principles and applications. Springer-Verlag New York, Inc. Secaucus, NJ, USA (2003)